



Lung cancer progression alters lung and gut microbiomes and lipid metabolism

Mao Hagihara^{a,b,1}, Hideo Kato^b, Makoto Yamashita^b, Yuichi Shibata^b, Takumi Umemura^b, Takeshi Mori^b, Jun Hirai^b, Nobuhiro Asai^b, Nobuaki Mori^b, Hiroshige Mikamo^{b,*}

^a Department of Molecular Epidemiology and Biomedical Sciences, Aichi Medical University, Nagakute, 480-1195, Japan

^b Department of Clinical Infectious Diseases, Aichi Medical University, Nagakute, 480-1195, Japan

ARTICLE INFO

Keywords:

Lung cancer
Microbiome
Metabolome
Lipid
Gut-lung axis

ABSTRACT

Despite advances in medical technology, lung cancer still has one of the highest mortality rates among all malignancies. Therefore, efforts must be made to understand the precise mechanisms underlying lung cancer development. In this study, we conducted lung and gut microbiome analyses and a comprehensive lipid metabolome analysis of host tissues to assess their correlation. Alternations in the lung microbiome due to lung cancer, such as a significantly decreased abundance of *Firmicutes* and *Deferribacterota*, were observed compared to a mock group. However, mice with lung cancer had significantly lower relative abundances of *Actinobacteria* and *Proteobacteria* and higher relative abundances of *Cyanobacteria* and *Patescibacteria* in the gut microbiome. The activations of retinol, fatty acid metabolism, and linoleic acid metabolism metabolic pathways in the lung and gut microbiomes was inversely correlated. Additionally, changes occurred in lipid metabolites not only in the lungs but also in the blood, small intestine, and colon. Compared to the mock group, mice with lung cancer showed that the levels of adrenic, palmitic, stearic, and oleic (a ω -9 polyunsaturated fatty acid) acids increased in the lungs. Conversely, these metabolites consistently decreased in the blood (serum) and colon. Leukotriene B4 and prostaglandin E2 exacerbate lung cancer, and were upregulated in the lungs of the mice with lung cancer. However, isohumulone, a peroxisome proliferator-activated receptor gamma activator, and resolvin (an ω -3 polyunsaturated fatty acid) both have anti-cancer effects, and were upregulated in the small intestine and colon. Our multi-omics data revealed that shifts in the microbiome and metabolome occur during the development of lung cancer and are of possible clinical importance. These results reveal one of the gut-lung axis mechanisms related to lung cancer and provide insights into potential new targets for lung cancer treatment and prophylaxis.

1. Introduction

Cancer is a major cause of death worldwide, and lung cancer has one of the highest mortality rates among all malignancies [1–3]. More than 80 % of all patients with lung cancer are diagnosed with non-small cell lung cancer (NSCLC) [4]. Despite considerable

* Corresponding author.

E-mail address: mikamo@aichi-med-u.ac.jp (H. Mikamo).

¹ Lead contact.

advances in medical technology, lung adenocarcinoma (LUAD), the most common type of NSCLC [4], is often diagnosed at an advanced stage [5], and its prognosis remains poor. Therefore, a better understanding of the precise mechanisms underlying the pathophysiology of LUAD is required.

Accumulating evidence has suggested that patients with colon cancer have different gut microbiome compositions compared to healthy volunteers, and some bacteria that comprise the human gut microbiome can be partially linked to the development of colon cancer [6] through the alteration of their immune and metabolic functions [7–10]. Additionally, a previous clinical study revealed that the lower airway dysbiotic signature was more prevalent in a stage IIIB–IV tumor–node–metastasis lung cancer group and was associated with poor prognosis [11]. These results suggest that lower airway dysbiosis affects lung cancer progression. However, the mechanisms by which the lung microbiome affects the progression of lung cancer are not fully understood [7].

Moreover, some studies have suggested the existence of a gut–lung axis, which can be related to the development and protection against certain diseases, including cancer, through metabolites derived from microorganisms, host tissues, and immune cells [8, 12–15]. Therefore, it is important to understand the role of the gut–lung axis in lung cancer progression. However, most studies on patients with lung cancer have focused on alterations in the microbiome and metabolites of either the lungs or gut [11].

Recent studies have revealed that lipids are associated with cancer progression [16–18], and that the gut microbiome affects host lipid metabolism [19,20]. As ω -3 polyunsaturated fatty acids (PUFAs) produced by colon tissue promote interferon production in the lungs, long-chain fatty acids affect the host immune system in a viral infection model [12]. Therefore, lipid metabolites may play an important role in connecting the lungs and gut to promote or inhibit lung cancer. However, the mechanisms by which lipid metabolites in the gut and lungs change in response to lung cancer and affect the disease remain unknown.

Therefore, comprehensive metagenomic and lipid metabolome analyses may provide an effective approach to understanding lung cancer development through associated changes in the lung and gut environments. To investigate these relationships, we conducted an *in vivo* study using a lung cancer model.

2. Materials and methods

2.1. Mice

Pathogen-free female C57BL/6J mice (14–15 weeks old), weighing approximately 30 g, were obtained from Charles River Laboratories Japan, Inc. (Yokohama, Japan). The mice were maintained and administered food and water *ad libitum*, as previously described [12]. This *in vivo* study was performed in accordance with the ARRIVE guidelines 2.0 (<https://arriveguidelines.org>), Japanese College of Laboratory Animal Medicine publication guide (<https://www.jalam.jp/>), and American Veterinary Medical Association guidelines (<https://www.avma.org>). This study was reviewed and approved by the ethics committee of Aichi Medical University (2022-50).

We prepared 30 mice with Lewis lung carcinoma (LLC) cells injected (plus 10 mice in the mock group) to evaluate the body weight and survival ratio. Additionally, we injected 50 mice with LLC cells ($n = 5, 5, 5, 5, 10,$ and 20 for days $0, 7, 14, 21, 28,$ and 32 sampling points) to evaluate tumor colon number, lung weights, and tumor volumes, 20 mice to evaluate the lung/colon microbiome ($n = 5, 5,$ and 10 for mock group, day $21,$ and day 28), and 27 mice to evaluate lipid metabolites ($n = 7$ and 20 for mock group and day 28).

2.2. Cell culture

The mouse LLC cell line (CRL-1642) was purchased from the American Type Culture Collection (ATCC, Manassas, VA, USA). Dulbecco's Modified Eagle's medium was obtained from ATCC (Manassas, VA, USA). Fetal bovine serum was obtained from Gibco (Waltham, MA, USA). Penicillin–streptomycin stocks were obtained from Wako (Osaka, Japan). The cells were cultured at $37\text{ }^{\circ}\text{C}$ in a humidified atmosphere containing 5% CO_2 .

2.3. Treatment of mice

According to the methods used in previous studies [21], LLC cells (1×10^6) suspended in $100\text{ }\mu\text{L}$ of phosphate-buffered saline (PBS) were injected into the tail vein of C57BL/6J female mice under anesthesia on day 0 using a 29-G syringe needle. At each time point (days $0, 7, 14, 21, 28,$ and 32 after tail vein injection of LLC cells), the mice were sacrificed by cervical dislocation following exposure to saturated CO_2 . Fecal samples from colonic tissue and bronchoalveolar lavage fluid (BALF) were collected from the mice on days $0, 21,$ and 28 and used for microbiome analysis. The BALF was collected using PBS (0.5 mL) as described previously [19]. We could not analyze the lung and gut microbiomes on day 32, because only a few mice injected with LLC cells survived. The lung, blood (via cardiopuncture), small intestine, and colonic tissues were collected on for lipid metabolome analysis on day 28. Because some mice died between sampling points, we failed to inject the LLC cells via the tail vein and gather adequate amounts of bacterial genes from BALF samples; therefore, the number of mice at each time point was different.

2.4. Assessment of physiological condition

During the study period, the mice were monitored daily. Weight loss was assessed on days $0, 7, 14, 21, 28,$ and 32 . These data were reported as the percentage of weight loss from the initial body weight (day 0) [12]. At each time point, metastases to the lungs, spleen, kidneys, liver, and intestines were monitored. Subsequently, the lungs were weighed, and the number of tumor colonies and lung size

were measured. Each tumor volume was calculated according to equation $V = (\text{length} \times \text{width}^2)/2$, and summarized for each mouse [22].

2.5. Pathologic evaluation

In this *in vivo* study, lung tissues were evaluated for histological changes, as previously described [12]. The lungs fixed with 10 % neutral buffered formalin were embedded in paraffin, cut into 3- μm sections, and stained with hematoxylin and eosin for histological analysis using light microscopy.

2.6. Lung and gut microbiome analyses

Microbiome analysis was conducted, according to methods described in a previous study, with small modifications [12,19,20,23]. The BALF and fecal samples were used to characterize the microbiome compositions of the lungs and colon. Meta 16S rRNA gene sequencing polymerase chain reaction was performed to the hypervariable V3–V4 region of the 16S rRNA gene using Ex Taq Hot Start (TAKARA Bio, Shiga, Japan), Illumina forward primer 50-AATGATACGGGACCACCGAGATCTACAC (adaptor sequence) + barcode (eight bases) + ACACTCTTCCCTACACGACGCTCTTCCGATCT (sequence primer) + CCTACGGGNGGCWGCAG-30 (341F), and the Illumina reverse primer 50-CAAGCAGAAGACGGCATACGAGAT (adaptor sequence) + barcode (eight bases) + GTGACTGGAGTT-CAGACGTGTGCTCTTCCGATCT (sequence primer) + GACTACHVGGGTATCTAATCC-30 (805R). A Quantus Fluorometer and QuantiFluor dsDNA System (Promega Corporation, Madison, WI, USA) were used to quantify DNA, and the samples were then prepared by pooling equal amounts of amplified DNA and sequenced using the MiSeq Reagent Kit V3 (600 cycles) (Illumina, San Diego, CA, USA).

The 16S rRNA sequence data generated by the MiSeq sequencer (Illumina) were processed using the Quantitative Insights into Microbial Ecology pipeline (QIIME 2) (<https://docs.qiime2.org/2020.6/>). Sequences with an average quality value < 20 were excluded. Additionally, α -diversity was calculated using QIIME 2. To compare the microbial composition between samples, β -diversity was measured by calculating the weighted UniFrac distances using QIIME 2 default scripts. Principal coordinate analysis (PCoA) was applied to the resulting distance matrices to generate two-dimensional plots.

2.7. Predictive functional profiling of gut microbial communities (PICRUSt)

To gain more insight into the metagenomics-based function of the microbiome in each group of mice, Phylogenetic Investigation of Communities by Reconstruction of Unobserved States (PICRUSt) v2.4.1 was used, as previously described [19]. The predicted data were collapsed into hierarchical categories (KEGG-Level-3), and the relative abundances of lung and gut metabolic functions were calculated using R software. The Kruskal-Wallis test was used for statistical analyses. Differentially expressed compounds with a linear discriminant analysis (LDA) score $p < 0.05$ using the Benjamini-Hochberg method were considered statistically significant.

2.8. Long-chain lipid metabolome analysis

Long-chain lipid metabolomic analysis was conducted as described previously, with minor modifications [12,19,20]. Briefly, the lungs, blood (serum), small intestine, and colon were sampled from the mice and immediately cryopreserved (stored at -80°C). The lungs, small intestine, and colon were lyophilized, and 10 mg was weighed after ball milling. Alternatively, 180 mL of methanol was added to 20 mL of the blood sample, and the mixture was vortexed for 1 min. We used a Vanquish ultra-high-performance liquid chromatography (UHPLC) system (Thermo Fisher Scientific), Q Exactive Focus (Thermo Fisher Scientific), with an electrospray ionization device, liquid chromatography-tandem mass spectrometry (LC-MS/MS), and Orbitrap LC-MS/MS analyses using an Acclaim RSLC120 C18 (Thermo Fisher Scientific) instrument to conduct the analysis.

Orbitrap LC-MS/MS analyses were performed in negative ion mode. Mobile phase A consisted of MilliQ and 0.1 % formic acid (Kanto Chemical Co., Inc., Tokyo, Japan). Acetonitrile (Kanto Chemical Co., Inc.) was used as mobile phase B. Two microliters of the sample was injected and measured. Gradient elution was applied at a flow rate of 400 $\mu\text{L}/\text{min}$ using the following time program: 0–0.5 min 20 % B, 0.5–15.0 min linear increase to 98 % B, 15.0–25.0 min remained at 98 % B, and 25.0–32.0 min linear decline to 20 % B.

Measured raw data were assigned to lipid metabolites by lipid MS/MS library as mentioned above after normalization, filtering, alignment, and peak identification using Compound Discoverer (Thermo Fisher Scientific) Version 3.1.

2.9. Quantification and statistical analysis

Quantification and statistical analyses were performed as described previously [12]. Data are presented as mean \pm standard deviation. Unless otherwise stated, all statistical analyses were performed using GraphPad Prism version 9 (GraphPad Software, San Diego, CA, USA). The Mann–Whitney U test (non-parametric) or independent samples t -test (parametric) was used to evaluate differences between two groups. For multiple group comparisons, statistical analysis was performed using the Kruskal–Wallis test (non-parametric), followed by the Dunn's test as a post-hoc test, or one-way analysis of variance (parametric), followed by the Bonferroni correction. The Kaplan–Meier curves and log-rank tests were used to perform survival analysis and to compare the groups.

3. Results

3.1. Lewis lung carcinoma cells selectively metastasize to the lungs and cause lung cancer

To evaluate whether LLC cells selectively metastasized to the lungs and underwent tumorigenesis, we injected the LLC cells (1×10^6) into the tail vein on day 0 (Fig. 1A). The LLC cell-injected mice showed a significant decrease in weight on days 28 and 32 compared with the mock group (Fig. 1B). The survival rates of the LLC cell-injected mice were significantly lower than those of the mock group (Fig. 1C). Although we did not observe tumor colonies in the spleen, liver, kidneys, or intestines of the LLC cell-injected mice, the number of tumor colonies in the lungs and volume of lung tumors increased during the study period (Fig. 1D and E). Additionally, the LLC cell-injected mice had significantly heavier lungs on days 28 and 32 than those in the LLC cell-injected mice on day 0 (Fig. 1F). Compared with the mock group, the LLC cell-injected mice showed thickening and broadening of the alveolar septa accompanied by infiltration of inflammatory cells on histological examination of the lungs (Fig. 1G). These results suggested that the injected the LLC cells metastasized to the lungs with high selectivity, and progressed to lung cancer during the study period. Hence, we used the LLC cell-injected mice as a lung cancer model.

3.2. Lung cancer alters lung and gut microbiomes

To reveal the impact of lung cancer on the lung and gut microbiomes, we conducted microbiome analysis on days 21 and 28

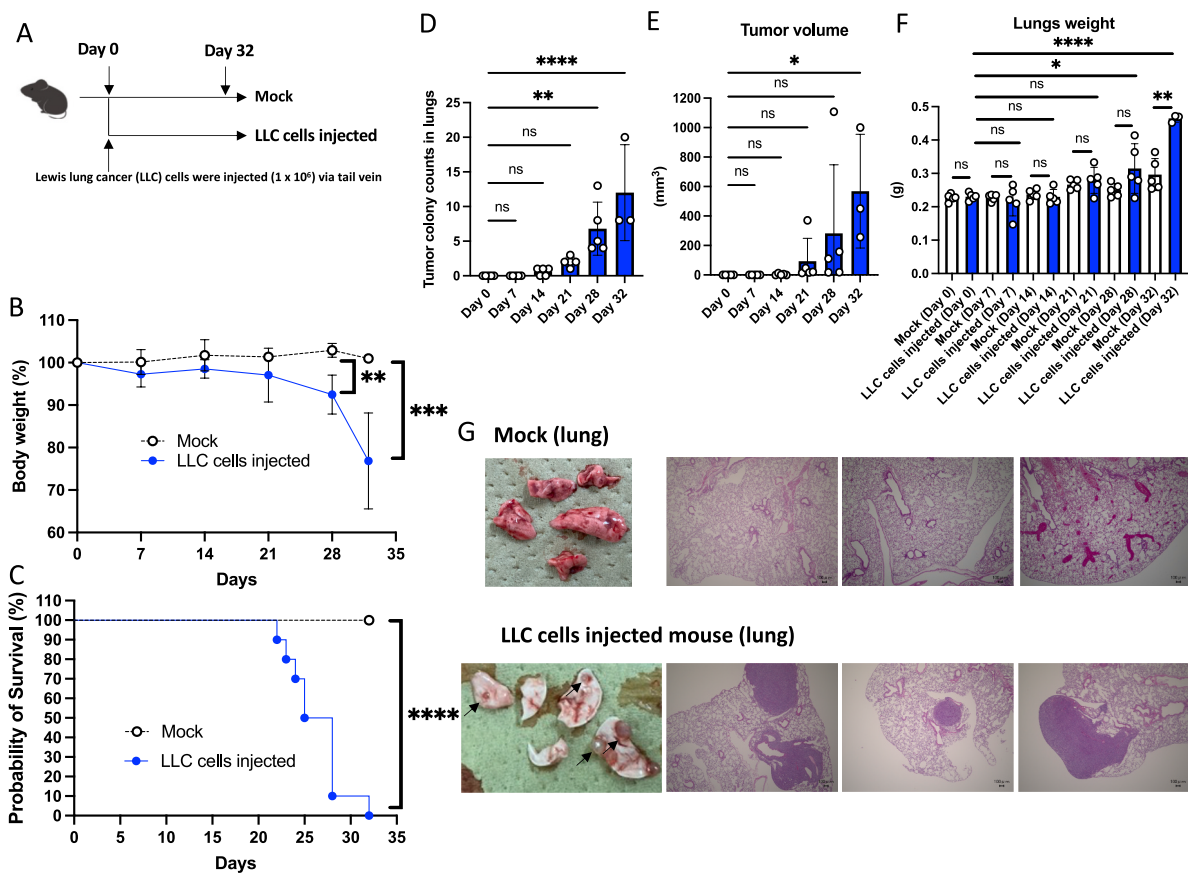


Fig. 1. Lewis lung cancer (LLC) cells metastasize selectively to the lungs and cause lung cancer

(A) C57BL/6J mice received LLC cells (1×10^6) via tail injection.

(B and C) body weight (B) results are presented as mean \pm standard deviation (SD) and survival rate (C). Mock, $n = 10$; LLC cell-injected mice, $n = 30$.

(D, E, and F) Tumor colony counts in the lungs (D), tumor volume in the lungs (E), weight of the lungs (F). Mock group mice and the LLC cell-injected mice were sacrificed on days 0, 7, 14, 21, 28, and 32 ($n = 5$ or 3). Results are presented as mean \pm SD. Each dot represents an individual mouse.

(G) Representative lung histological images on day 28 after LLC cell injection (scale bar, 100 μ m at the bottom right). Black arrow shows tumor nodules (left). Three images from right were derive from different mice, respectively.

Results were considered statistically significant if the p value was <0.05 (**** $p < 0.001$, *** $p < 0.001$, ** $p < 0.01$).

(Fig. 2A) to determine changes in the murine lung, and gut microbiomes at the phylum level. Bar graphs showed the mean abundance of the bacterial families (Fig. 2B). Mice with lung cancer showed a significantly decreased abundance of *Firmicutes* and *Deferribacterota* in the lung microbiome compared to the mock group. However, mice with lung cancer showed a significantly lower relative abundance of *Actinobacteria* and *Proteobacteria* and a higher relative abundance of *Cyanobacteria* and *Patescibacteria* in the gut microbiome than the mock group.

Patients with lung cancer have different lung and gut microbes compared with healthy volunteers [7]. In this study, we found that mice with lung cancer also had different lung and gut microbiomes from the mock group (Fig. 2C and D). Lung cancer mice showed decreased α -diversity in the lung microbiome compared with the mock group on day 28, but the difference was not significant (Fig. 2C). Conversely, lung cancer mice had increased α -diversity in the gut microbiome (Fig. 2C). Additionally, PCoA showed that lung cancer altered the composition of bacterial communities in the lungs and gut (Fig. 2D). On day 28, the lung microbiome in the lung cancer mouse group had significantly clustered bacterial communities compared to that in the mock group. Similarly, on Days 21 and 28, the gut microbiome in the lung cancer group showed significant clustering of bacterial communities and divergence from the mock group.

At the genus level, the lung cancer mice showed a significantly different relative abundance of 7 and 13 species in the lung and gut microbiomes on days 21 and 28, respectively, compared with the mock group (Figs. S2A and S2B). In the lung microbiome, *Mucispirillum* spp., *Bacillus* spp., *Roseburia* spp., *Blautia* spp., and *Oscillibacter* spp. showed lower relative abundance in the lung cancer mouse group than those in the mock group, whereas *Muribaculaceae* and *Enterobacteriaceae* showed higher relative abundance in the lung cancer mouse group (Fig. S2A). Conversely, in the gut microbiome, *Enterorhabdus* spp., *Parvibacter* spp., *Muribaculaceae*, *Desulfobacteriaceae*, *Ligilactobacillus* spp., *Parasutterella* spp., and *Eubacterium* brachy showed lower relative abundance in the lung cancer mouse group than that in the mock group. However, RF39, *Candidatus saccharimonas*, *Gastranaerophilales* spp., *Lachnospiraceae*, *Monoglobus*

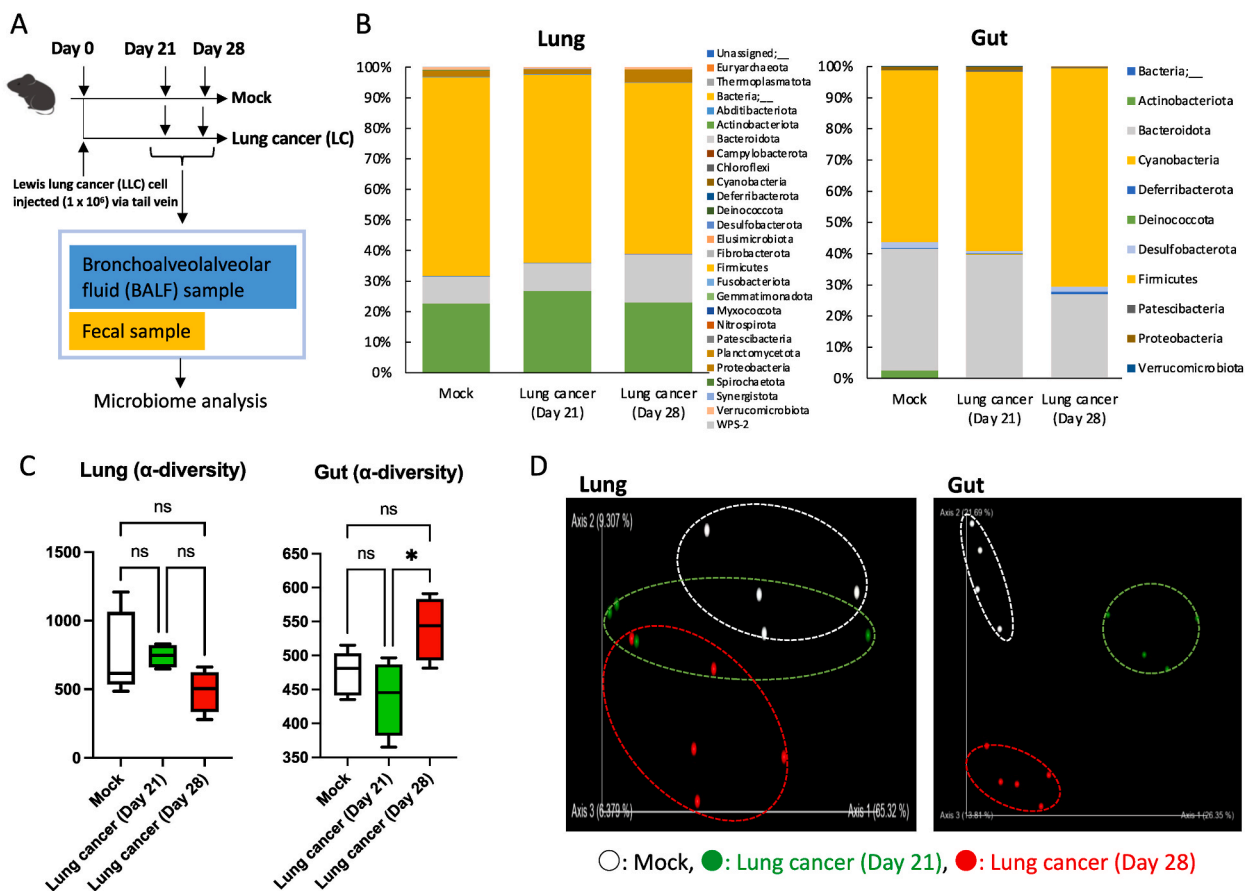


Fig. 2. Lung cancer alters the lung and gut microbiomes

(A) C57BL/6J mice received Lewis lung cancer (LLC) cells (1×10^6) via tail injection. Mock, $n = 5$; lung cancer mice were sacrificed on days 21 ($n = 4$) and 28 ($n = 4$).

(B) Bacterial composition in the lungs (left) and gut (right) at the phylum level.

(C) Comparison of the Chao1 index of different groups. The box and whiskers represent the smallest and largest values, with the median in the center of each box. Results were considered statistically significant if the p value was < 0.05 (* $p < 0.05$; ns indicates not significant).

(D) Principal coordinates analysis (PCoA) based on weighted UniFrac distances among three groups (mock, lung cancer sacrificed on day 21, and lung cancer sacrificed on day 28). Each dot represents an individual mouse. See also Fig. S2.

spp., and *Ruminococcaceae* were significantly more abundant in the lung cancer group than those in the control group (Fig. S2B).

3.3. Lung cancer alter metabolic functions in the lung and gut microbiomes

To reveal the alterations in metabolic functions in the lung and gut microbiomes, we used the PICRUSt analysis and found that lung cancer mice on days 21 and 28 showed significantly different relative abundances of 5 and 26 metabolic pathways in the lung and gut microbiomes, respectively, compared with the mock group (Fig. 3A). In the lung microbiome, “alanine, aspartate, and glutamate metabolism,” “homologous recombination,” “retinol metabolism,” “fatty acid metabolism,” and “linoleic acid metabolism” were significantly altered in the lung cancer mouse group compared to those in the mock group (Fig. 3B). Retinol metabolism in the lung microbiome was significantly activated, whereas metabolic function in the gut microbiome was significantly attenuated in the lung cancer mouse group (Figs. 3B and S3A). Similar trends were observed for the fatty acid and linoleic acid metabolisms in the lung and gut microbiomes. The activation of these metabolic pathways in the lung and gut microbiomes was inversely correlated (Figs. 3B and S3A).

3.4. Lung cancer changes lipid metabolic profiles in host lung, blood, small intestine, and colon

To determine how lung cancer affects lipid metabolism in the host, comprehensive lipid metabolite analyses of the colon, small intestine, blood (serum), and lungs were conducted (Fig. 4A). Structural isomers, including 519, 941, 619, and 463 lipid metabolites, were assigned after comparison with fragment libraries. The PCoA showed that lung cancer altered the lipid metabolite composition in

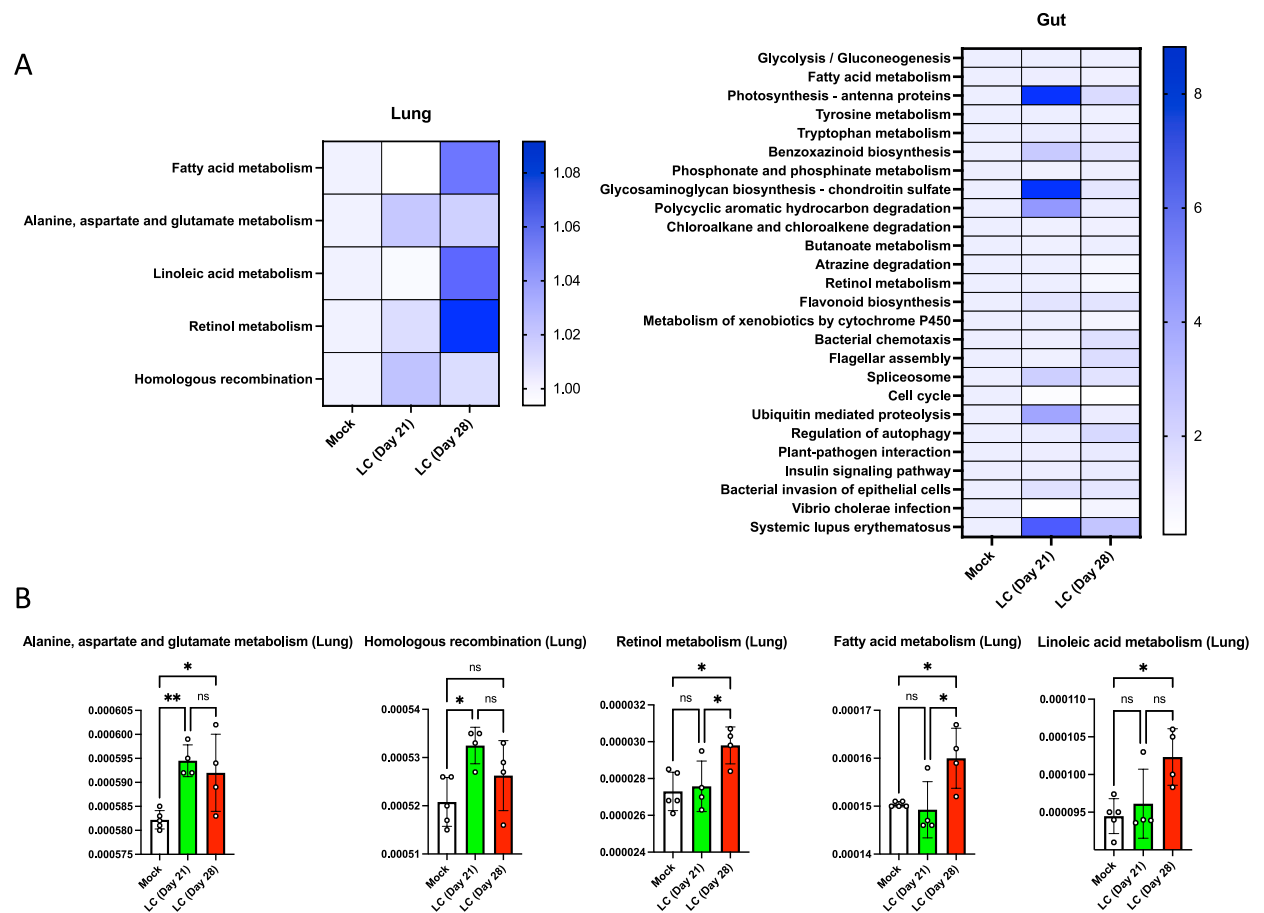


Fig. 3. Lung cancer alters metabolism in the lungs

(A) Heatmap representing the ratio of the mock group to the relative abundance of the metabolic functions in the lung and gut microbiome. C57BL/6J mice received LLC cells (1×10^6) via tail injection. Mock, $n = 5$; lung cancer mice sacrificed on days 21 ($n = 4$) and 28 ($n = 4$). (B) Effect of lung cancer on relative abundance of the metabolic functions in the lung microbiome. Results are presented as mean \pm standard deviation (SD). Each dot represents an individual mouse. Results were considered statistically significant if the p value was < 0.05 (** $p < 0.01$, * $p < 0.05$; ns indicates not significant). See also Fig. S3.

the lungs and gut (Figs. S4A–S4D). Additionally, in the mice with lung cancer, 18, 23, 21, and 17 metabolites in the colon, small intestine, blood (serum), and lungs, respectively, showed significantly different peak intensities compared to those of the mock group (Fig. 4B–E). Most metabolites in the lungs were upregulated in the lung cancer mice group compared to those in the mock group, whereas most metabolites in the blood (serum), small intestine, and colon were downregulated in the lung cancer mice group. The levels of adrenic (an ω -6 PUFA), palmitic, stearic, and oleic (an ω -9 PUFA) acids increased in the lungs. Conversely, their levels consistently decreased in the blood (serum) and colon. Additionally, leukotriene B4 (LTB4) and prostaglandin E2, which exacerbate lung cancer [24–27], are upregulated in the lungs. However, isohumulone, which is a peroxisome proliferator-activated receptor gamma (PPAR γ) activator [28], and resolvin (an ω -3 PUFA), one of the specialized pro-resolving mediators (SPMs), which both have anti-cancer effects, were upregulated in the small intestine and colon [17,18,29–31].

4. Discussion

In this study, we confirmed that our *in vivo* model can be used as a lung cancer model. The LLC cells injected via the tail vein showed high selectivity for lungs and lung cancer progression over time during the study period. We used these mice as the lung cancer group and conducted microbiome and lipid metabolic analyses and found that lung cancer affects microbiomes not only in the lungs but also in the gut.

A clinical study suggested that lower airway dysbiosis may be related to lung cancer progression [11]. Our *in vivo* study showed that the lung microbiome changed with lung cancer progression. Then, the alterations in α -diversity in the lung and gut microbiomes showed an inverse correlation. The microbiome affects the host lipid metabolism [19,20]. Hence, we hypothesized that some species affected the host lipid metabolism, as suggested by our PICRUSt analysis. In fact, we previously reported increased lipid metabolism after microbiota diversity decreased [19,20,23]. Additionally, as human can not produce ω -3 PUFAs, such as docosahexaenoic acid (DHA) and eicosatetraenoic acid (EPA), are parent compounds of resolvin, by themselves, microbiome plays an important role to produce PUFAs [17,18,29,30]. Therefore, we hypothesized that small changes in lipid metabolism could be caused by microbiome alterations.

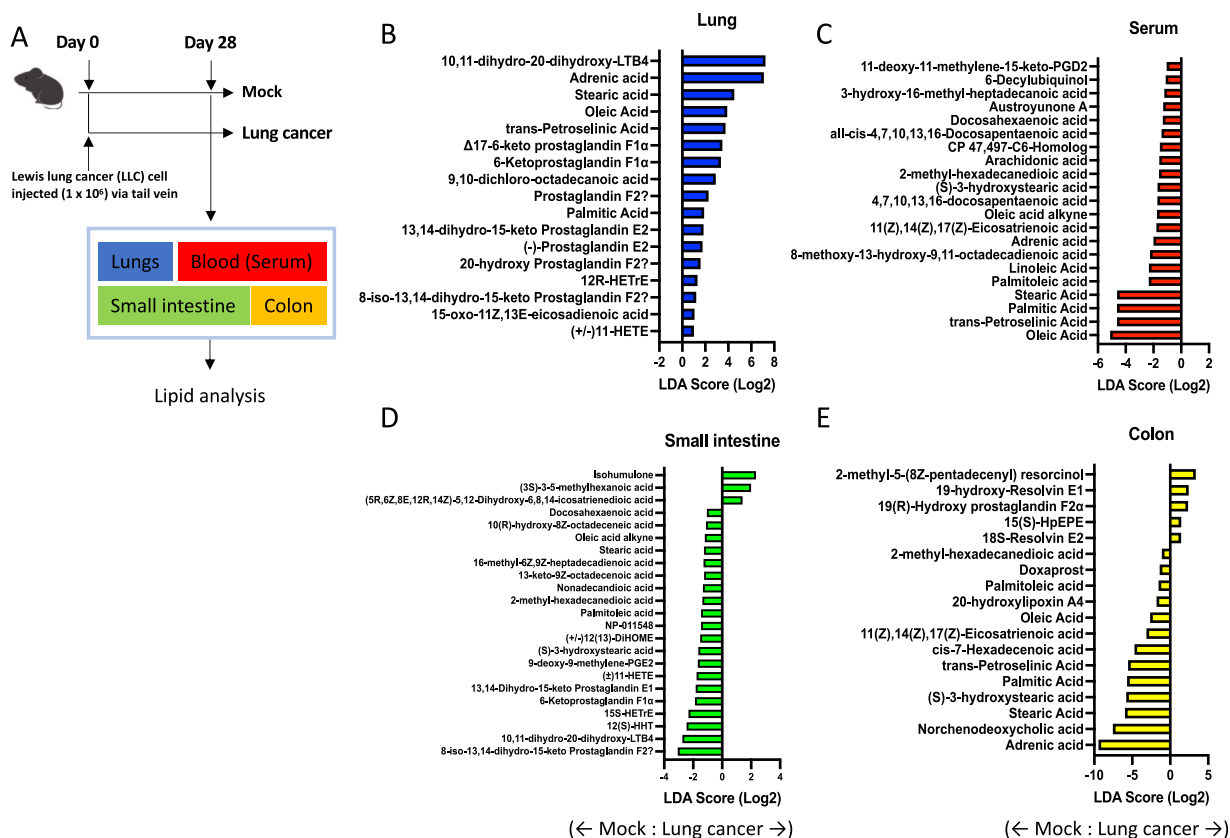


Fig. 4. Lung cancer changes metabolic profiles in host lung, blood, small intestine, and colon

(A) C57BL/6J mice received LLC cells (1×10^6) via tail injection. Mock, $n = 7$; lung cancer mice sacrificed on day 28, $n = 8$.

(B, C, D, and E) Linear discriminant analysis (LDA) score (Log2) of lipid metabolites that show significantly different peak areas between the mock and lung cancer mouse groups in the lungs (B), blood (serum) (C), small intestine (D), and colon (E). Results are presented as mean of LDA score. See also Fig. S4.

Among these bacterial species, showed significantly different relative abundance between the lung cancer and mock groups, *Muribaculaceae* consume mucin [32,33], *Mucispirillum* spp. inhabit the mucin layer [34], and *Roseburia* spp. are butyrate-producing bacteria that promote mucin production [35,36]. Additionally, *Blautia* spp. and *Oscillibacter* spp. are decreased in colorectal cancer and inflammatory bowel disease (IBD) owing to the gut [37–40]. Hence, the lung microbiome alterations found in this study suggest the destruction of the mucin layer and inflammation in the lungs.

In contrast, in the gut microbiome, *Entororhabdus* spp. and *Parasutterella* spp. are increased in patients with IBD [41–43]. However, in this study, the lung cancer mouse group showed decreased abundance in the gut microbiome. Additionally, *Muribaculaceae* was the only phylum that changed significantly in abundance in both the lung and gut microbiomes, and the relative abundances in the lung and gut microbiomes showed an inverse correlation. Therefore, they can affect the progression of lung cancer and can be used as markers to predict lung cancer. However, further research is needed to clarify the underlying mechanisms.

As next step of this study, because microbiome-derived metabolites act both as nutrients and as messenger molecules to the host, we focused on the alterations of metabolic functions in the resident microbiome to elucidate how lung cancer modulation of the lung and gut microbiota affected their metabolic functions during lung cancer progression [7,9,11]. Consequently, “retinol metabolism” in the lung microbiome was significantly activated in mice with lung cancer, whereas the metabolic function in the gut microbiome was significantly attenuated. A higher dietary retinol intake is associated with the incidence of lung cancer [44]. Therefore, it can be used as a marker for lung cancer; however, further studies are required to confirm this hypothesis.

Although we observed enhanced “alanine, aspartate, and glutamate metabolism” in the lung microbiome, cancer cells activated glutamine metabolism [45], which can lead to the consumption of butyrate as a source of glutamine in the lungs [46,47]. Therefore, the shortage of butyrate, which is the main source of mucin, leads to destruction of the mucin layer in the lungs and causes inflammation [36]. The metabolism also plays a role in lipid metabolism, particularly in cancer cells [47]. These metabolic enhancements were consistent with the upregulation of certain lipid metabolites in the lungs.

Furthermore, we observed significantly enhancements in “fatty acid metabolism,” and “linoleic acid metabolism” in lung microbiome with lung cancer, and they showed inverse correlation between the lung and gut microbiomes. Linoleic acid is a source of DHA, EPA, and arachidonic acids [48,49]. Therefore, we speculated that these alterations in metabolic functions in the lung and gut microbiomes could affect the progression of lung cancer through the upregulation of lipid metabolites.

We found that most fatty acid metabolites were upregulated in the lung microbiome of the lung cancer group compared to the mock group, whereas most fatty acid metabolites in the blood (serum), small intestine, and colon were downregulated.

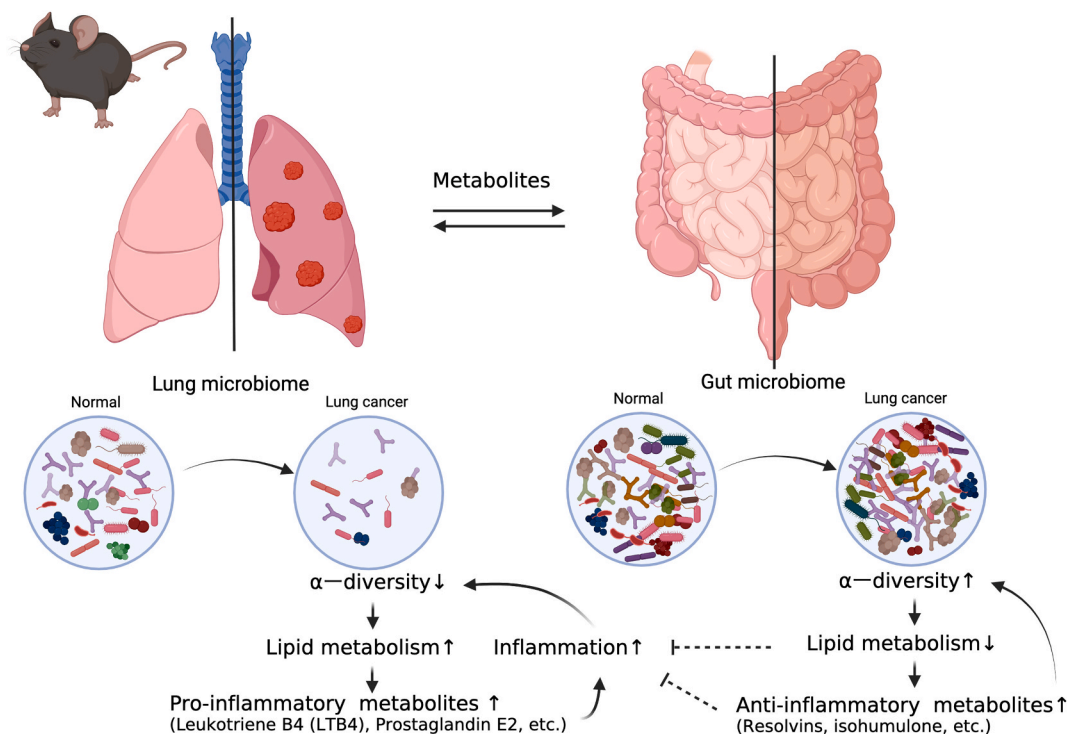


Fig. 5. Proposed mechanisms to show the correlation between the lung and gut in lung cancer mice

Lung cancer induces inflammation and changes in the microbiome. These factors promote lipid metabolism in the lungs. Additionally, lung cancer upregulates ω -6 polyunsaturated fatty acids (PUFAs) (adrenic acid), pro-inflammatory lipid mediators, and their sources, long-chain fatty acids, such as oleic, palmitic, and stearic acids, to promote lung cancer progression. However, the gut decreases the production of these metabolites, thereby reducing their supply to the lungs. Instead, the gut upregulates anti-inflammatory lipid metabolites, such as resolvins. Alterations in lipid metabolism can also affect the gut microbiome.

Among lipid metabolites, ω -3 and ω -6 PUFAs can affect the tumor formation and play an essential role in inhibiting migration and invasion [16–18]. Higher ω -6 PUFAs are a potential mediator of cancer prognosis [16], whereas ω -3 PUFAs can help prevent cancer [17,18]. In this study, the levels of adrenic acid (an ω -6 PUFA), palmitic acid, stearic acid, and oleic acid (ω -9 PUFAs) increased in the lungs of lung cancer mice. Conversely, their levels consistently decreased in the blood (serum) and colon. In contrast, LTB4 and prostaglandin E2, which aggravate lung cancer [25,27], are upregulated in the lungs. However, isohumulone, which is a PPAR γ activator [28], and resolvin (an ω -3 PUFA and SPM) [48], which has anti-inflammatory effects, were upregulated in the small intestine and colon, respectively [18,29].

Collectively, our data suggest that lung cancer causes inflammation and changes in the lung microbiome, which activate lipid metabolic functions in the lungs, with some support from the lung microbiome. In lung cancer, ω -6 PUFAs (such as adrenic acid), pro-inflammatory lipid mediators, and their source long-chain fatty acids, such as oleic, palmitic, and stearic acids, are upregulated, and this is associated with lung cancer progression [16–18]. However, their production in the gut is reduced, which in turn reduces their supply to the lungs. Instead, the gut upregulates anti-inflammatory lipid metabolites, such as resolvins. These alterations in lipid metabolism can affect gut microbiome diversity and composition (Fig. 5).

Our study suggests a lung-gut axis mechanism. However, this study has some limitations. First, the human microbiome differs from the mouse microbiome [50]. Clinical studies conducted in humans have shown an increase in *Veilonella* spp. In the lung microbiome and enhanced inflammatory responses [11]. However, the same results were not obtained in the present study. Further studies are required to investigate whether these results can be replicated in humans. Second, we focused only on host lipid metabolites because the PICRUST analysis suggested that the metabolic activity of lipid metabolism in the lung and gut microbiomes was inversely correlated. Nutrients other than lipids may also be involved in the progression of lung cancer. Additionally, this study conducted a comprehensive lipid analysis, but we did not reveal the roles of specific lipid metabolites in cancer progression and microbiomes in the host or the correlations between metabolic products and microbial categories in the microbiomes. Further studies are required to determine the most important bacterial species and lipid metabolites that affect lung cancer progression. Finally, our study used only female mice, as our referenced previous study used female mice [21]. Hence, further studies are required to evaluate the differences between female and male mice.

5. Conclusion

Our multi-omics data showed that shifts in the microbiome and metabolome occur during the development of lung cancer, which are of prognostic importance. These results revealed a gut-lung axis mechanism related to lung cancer and provided novel insights into potential targets for lung cancer treatment and prophylaxis.

Inclusion and diversity

We support inclusive, diverse, and equitable conduct of research.

CRediT authorship contribution statement

Mao Hagihara: Writing - review & editing, Writing - original draft, Validation, Methodology, Investigation, Formal analysis, Data curation, Conceptualization. **Hideo Kato:** Formal analysis. **Makoto Yamashita:** Supervision, Methodology. **Yuichi Shibata:** Writing - review & editing. **Takumi Umemura:** Writing - review & editing. **Takeshi Mori:** Investigation. **Jun Hirai:** Writing - review & editing. **Nobuhiro Asai:** Writing - review & editing. **Nobuaki Mori:** Writing - review & editing. **Hiroshige Mikamo:** Resources, Funding acquisition.

Declaration of AI and AI-assisted technologies in the writing process

The authors did not use AI or AI-assisted technologies during the writing process.

Declaration of competing interest

The authors declare that they have no known competing financial interests or personal relationships that could have appeared to influence the work reported in this paper.

Acknowledgments

We thank the Division of Laboratory Animal Research (Aichi Medical University) for providing the facilities for performing the animal experiments, and the Division of Advanced Research Promotion (Aichi Medical University) for technical instructions and assistance.

Appendix A. Supplementary data

Supplementary data to this article can be found online at <https://doi.org/10.1016/j.heliyon.2023.e23509>.

References

- [1] F. Bray, J. Ferlay, I. Soerjomataram, R.L. Siegel, L.A. Torre, A. Jemal, Global cancer statistics 2018: GLOBOCAN estimates of incidence and mortality worldwide for 36 cancers in 185 countries, *CA Cancer J. Clin.* 68 (2018) 394–424, <https://doi.org/10.3322/caac.21492>.
- [2] Z. Wu, Y. Tian, Q. Yu, H. Li, Z. Tian, H. Jiang, D. Tian, X. Yang, The expression and correlation between chemokine CCL7 and ABCE1 in non-small cell lung cancer, *Exp. Ther. Med.* 16 (2018) 3004–3010, <https://doi.org/10.3892/etm.2018.6568>.
- [3] R.L. Siegel, K.D. Miller, N.S. Wagle, A. Jemal, Cancer statistics, 2023, *CA Cancer J. Clin.* 73 (2023) 17–48, <https://doi.org/10.3322/caac.21763>.
- [4] J. Ferlay, I. Soerjomataram, R. Dikshit, S. Eser, C. Mathers, M. Rebelo, D.M. Parkin, D. Forman, F. Bray, Cancer incidence and mortality worldwide: sources, methods and major patterns in GLOBOCAN 2012, *Int. J. Cancer* 136 (2015) E359–E386, <https://doi.org/10.1002/ijc.29210>.
- [5] D.S. Ettinger, D.E. Wood, C. Aggarwal, D.L. Aisner, W. Akerley, J.R. Bauman, A. Bharat, D.S. Bruno, J.Y. Chang, L.R. Chirieac, NCCN guidelines insights: non-small cell lung cancer, version 1, *J. Natl. Compr. CancNetw.* 17 (2019) 1464–1472, <https://doi.org/10.6004/jnccn.2019.0059>.
- [6] S. Yachida, S. Mizutani, H. Shiroma, S. Shiba, T. Nakajima, T. Sakamoto, H. Watanabe, K. Masuda, Y. Nishimoto, M. Kubo, et al., Metagenomic and metabolomic analyses reveal distinct stage-specific phenotypes of the gut microbiota in colorectal cancer, *Nat. Med.* 25 (2019) 968–976, <https://doi.org/10.1038/s41591-019-0458-7>.
- [7] Y. Zhao, Y. Liu, S. Li, Z. Peng, X. Liu, J. Chen, X. Zheng, Role of lung and gut microbiota on lung cancer pathogenesis, *J. Cancer Res. Clin. Oncol.* 147 (2021) 2177–2186, <https://doi.org/10.1007/s00432-021-03644-0>.
- [8] N. Vallianou, D. Kounatidis, G.S. Christodoulatos, F. Panagopoulos, I. Karampela, M. Dalamaga, Mycobiome and cancer: what is the evidence? *Cancers* 13 (2021) 3149, <https://doi.org/10.3390/cancers13133149>.
- [9] S. Lozenov, B. Krastev, G. Nikolaeve, M. Peshevska-Sekulovska, M. Peruhova, T. Velikova, Gut microbiome composition and its metabolites are a key regulating factor for malignant transformation, metastasis and antitumor immunity, *Int. J. Mol. Sci.* 24 (2023) 5978, <https://doi.org/10.3390/ijms24065978>.
- [10] C. Campbell, M.R. Kandalgaonkar, R.M. Golonka, B.S. Yeoh, M. Vijay-Kumar, P. Saha, Crosstalk between gut microbiota and host immunity: impact on inflammation and immunotherapy, *Biomedicines* 11 (2023) 294, <https://doi.org/10.3390/biomedicines11020294>.
- [11] J.-C.J. Tsay, B.G. Wu, I. Sulaiman, K. Gershner, R. Schluger, Y. Li, T.-A. Yie, P. Meyn, E. Olsen, L. Perez, et al., Lower airway dysbiosis affects lung cancer progression, *Cancer Discov.* 11 (2021) 293–307, <https://doi.org/10.1158/2159-8290.CD-20-0263>.
- [12] M. Hagihara, M. Yamashita, T. Ariyoshi, S. Eguchi, A. Minemura, D. Miura, S. Higashi, K. Oka, T. Nonogaki, T. Mori, et al., Clostridium butyricum-induced ω -3 fatty acid 18-HEPE elicits anti-influenza virus pneumonia effects through interferon- λ upregulation, *Cell Rep.* 41 (2022), 111755, <https://doi.org/10.1016/j.celrep.2022.111755>.
- [13] F. Shoji, M. Yamaguchi, M. Okamoto, S. Takamori, K. Yamazaki, T. Okamoto, Y. Maehara, Gut microbiota diversity and specific composition during immunotherapy in responders with non-small cell lung cancer, *Front. Mol. Biosci.* 9 (2022), 1040424, <https://doi.org/10.3389/fmolb.2022.1040424>.
- [14] B.W. Haak, E.R. Littmann, J.-L. Chaubard, A.J. Pickard, E. Fontana, F. Adhi, Y. Gyaltsen, L. Ling, S.M. Morjarra, J.U. Peled, et al., Impact of gut colonization with butyrate-producing microbiota on respiratory viral infection following allo-HCT, *Blood* 131 (2018) 2978–2986, <https://doi.org/10.1182/blood-2018-01-828996>.
- [15] J.O. Kim, R. Balshaw, C. Trevena, S. Banerji, L. Murphy, D. Dawe, L. Tan, S. Srinathan, G. Buduhan, B. Kidane, et al., Data-driven identification of plasma metabolite clusters and metabolites of interest for potential detection of early-stage non-small cell lung cancer cases versus cancer-free controls, *Cancer Metabol.* 10 (2022) 16, <https://doi.org/10.1186/s40170-022-0>.
- [16] P.C. Haycock, C. Maria Borges, K. Burrows, R.N. Lemaitre, S. Burgess, N.K. Khankari, K.K. Tsilidis, T.R. Gaunt, G. Hemani, J. Zheng, et al., The association between genetically elevated polyunsaturated fatty acids and risk of cancer, *EbioMedicine* 91 (2023), 104510, <https://doi.org/10.1016/j.ebiom.2023.104510>.
- [17] A. Kantarci, S. Kansal, H. Hasturk, D. Stephens, T.E. Van Dyke, Resolvin E1 reduces tumor growth in a xenograft model of lung cancer, *Am. J. Pathol.* 192 (2022) 1470–1484, <https://doi.org/10.1016/j.ajpath.2022.07.004>.
- [18] X. Bai, J. Shao, S. Zhou, Z. Zhao, F. Li, R. Xiang, A.Z. Zhao, J. Pan, Inhibition of lung cancer growth and metastasis by DHA and its metabolite, RvD1, through miR-138-5p/FOXO1 pathway, *J. Exp. Clin. Cancer Res.* 38 (2019) 479, <https://doi.org/10.1186/s13046-019-1478-3>.
- [19] M. Hagihara, Y. Kuroki, T. Ariyoshi, S. Higashi, K. Fukuda, R. Yamashita, A. Matsumoto, T. Mori, K. Mimura, N. Yamaguchi, et al., Clostridium butyricum Modulates the microbiome to protect intestinal barrier function in mice with antibiotic-induced dysbiosis, *iScience* 23 (2020), 100772, <https://doi.org/10.1016/j.isci.2019.100772>.
- [20] T. Ariyoshi, M. Hagihara, S. Tomono, S. Eguchi, A. Minemura, D. Miura, K. Oka, M. Takahashi, Y. Yamagishi, H. Mikamo, Clostridium butyricum MIYAIRI 588 Modifies bacterial composition under antibiotic-induced dysbiosis for the activation of Interactions via lipid metabolism between the gut microbiome and the host, *Biomedicines* 9 (2021) 1065, <https://doi.org/10.3390/biomedicines9081065>.
- [21] D. Upreti, S. Ishiguro, N. Robben, A. Nakashima, K. Suzuki, J. Comer, M. Tamura, Oral administration of water extract from *eglena gracilis* alters the intestinal microbiota and prevents lung carcinoma growth in mice, *Nutrients* 14 (2022) 678, <https://doi.org/10.3390/nu14030678>.
- [22] T. Qiao, J. Zhao, X. Xin, Y. Xiong, W. Guo, F. Meng, H. Li, Y. Feng, H. Xu, C. Shi, et al., Combined pembrolizumab and bevacizumab therapy effectively inhibits non-small-cell lung cancer growth and prevents postoperative recurrence and metastasis in humanized mouse model, *Cancer Immunol. Immunother.* 72 (2023) 1169–1181, <https://doi.org/10.1007/s00262-022-03318-x>.
- [23] T. Ariyoshi, M. Hagihara, S. Eguchi, A. Fukuda, K. Iwasaki, K. Oka, M. Takahashi, Y. Yamagishi, H. Mikamo, Clostridium butyricum MIYAIRI 588-induced protectin D1 has an anti-inflammatory effect on antibiotic-induced intestinal disorder, *Front. Microbiol.* 11 (2020), 587725, <https://doi.org/10.3389/fmicb.2020.587725>.
- [24] J.H. Jang, D. Park, G.S. Park, D.W. Kwak, J. Park, D.Y. Yu, H.J. You, J.H. Kim, Leukotriene B4 receptor-2 contributes to KRAS-driven lung tumor formation by promoting interleukin-6-mediated inflammation, *Exp. Mol. Med.* 53 (2021) 1559–1568, <https://doi.org/10.1038/s12276-021-00682-z>.
- [25] T. Nosaka, T. Baba, Y. Tanabe, S. Sasaki, T. Nishimura, Y. Imamura, H. Yurino, S. Hashimoto, M. Arita, Y. Nakamoto, et al., Alveolar macrophages drive hepatocellular carcinoma lung metastasis by generating leukotriene B4, *J. Immunol.* 200 (2018) 1839–1852, <https://doi.org/10.4049/jimmunol.1700544>.
- [26] M. Zhao, Y. Wang, Y. Zhao, S. He, R. Zhao, Y. Song, J. Cheng, Y. Gong, J. Xie, Y. Wang, et al., Caspase-3 knockout attenuates radiation-induced tumor repopulation via impairing the ATM/p53/Cox-2/PGE2 pathway in non-small cell lung cancer, *Aging (Albany NY)* 12 (2020) 21758–21776, <https://doi.org/10.18632/aging.103984>.
- [27] J. Yang, X. Wang, Y. Gao, C. Fang, F. Ye, B. Huang, L. Li, Inhibition of PI3K-AKT signaling blocks PGE2-induced COX-2 expression in lung adenocarcinoma, *Oncotargets Ther.* 13 (2020) 8197–8208, <https://doi.org/10.2147/OTT.S263977>.
- [28] H. Yajima, E. Ikeshima, M. Shiraki, T. Kanaya, D. Fujiwara, H. Odai, N. Tsuboyama-Kasaoka, O. Ezaki, S. Oikawa, K. Kondo, Isohumulones, bitter acids derived from hops, activate both peroxisome proliferator-activated receptor alpha and gamma and reduce insulin resistance, *J. Biol. Chem.* 279 (2004) 33456–33462, <https://doi.org/10.1074/jbc.M403456200>.
- [29] H. Yin, Y. Liu, H. Yue, Y. Tian, P. Dong, C. Xue, Y.T. Zhao, Z. Zhao, J. Wang, DHA- and EPA-enriched phosphatidylcholine suppress human lung carcinoma 95D cells metastasis via activating the peroxisome proliferator-activated receptor γ , *Nutrients* 14 (2022) 4675, <https://doi.org/10.3390/nu14214675>.
- [30] L.D. Dwyer-Nield, D.G. McArthur, T.M. Hudish, L.I. Hudish, C. Mirita, K. Sompel, A.J. Smith, K. Alavi, M. Ghosh, D.T. Merrick, et al., PPARgamma agonism inhibits progression of premalignant lesions in a murine lung squamous cell carcinoma model, *Int. J. Cancer* 151 (2022) 2195–2205, <https://doi.org/10.1002/ijc.34210>.
- [31] N.D. Portela, C. Galván, L.M. Sanmarco, G. Bergero, M.P. Aoki, R.C. Cano, S.A. Pesoa, Omega-3-Supplemented fat diet drives immune metabolic response in visceral adipose tissue by modulating gut microbiota in a mouse model of obesity, *Nutrients* 15 (2023) 1404, <https://doi.org/10.3390/nu15061404>.
- [32] F.C. Pereira, K. Wasmund, I. Cobankovic, N. Jehmlich, C.W. Herbold, K.S. Lee, B. Sziranyi, C. Vesely, T. Decker, R. Stocker, et al., Rational design of a microbial consortium of mucosal sugar utilizers reduces Clostridiodes difficile colonization, *Nat. Commun.* 11 (2020) 5104, <https://doi.org/10.1038/s41467-020-18928-1>.

- [33] K.L. Ormerod, D.L.A. Wood, N. Lachner, S.L. Gellatly, J.N. Daly, J.D. Parsons, C.G.O. Dal'Molin, R.W. Palfreyman, L.K. Nielsen, M.A. Cooper, et al., Genomic characterization of the uncultured Bacteroidales family S24-7 inhabiting the guts of homeothermic animals, *Microbiome* 4 (2016) 36, <https://doi.org/10.1186/s40168-016-0181-2>.
- [34] B.R. Robertson, J.L. O'Rourke, B.A. Neilan, P. Vandamme, S.L.W. On, J.G. Fox, A. Lee, *Mucispirillum schaedleri* gen. nov., sp. nov., a spiral-shaped bacterium colonizing the mucus layer of the gastrointestinal tract of laboratory rodents, *Int. J. Syst. Evol. Microbiol.* 55 (2005) 1199–1204, <https://doi.org/10.1099/ijs.0.63472-0>.
- [35] P. Van den Abbeele, C. Belzer, M. Goossens, M. Kleerebezem, W.M. De Vos, O. Thas, R. De Weirtd, F.M. Kerckhof, T. Van de Wiele, Butyrate-producing *Clostridium* cluster XIVa species specifically colonize mucins in an in vitro gut model, *ISME J.* 7 (2013) 949–961, <https://doi.org/10.1038/ismej.2012.158>.
- [36] C.T. Brown, A.G. Davis-Richardson, A. Giongo, K.A. Gano, D.B. Crabb, N. Mukherjee, G. Casella, J.C. Drew, J. Ilonen, M. Knip, et al., Gut microbiome metagenomics analysis suggests a functional model for the development of autoimmunity for type 1 diabetes, *PLoS One* 6 (2011), e25792, <https://doi.org/10.1371/journal.pone.0025792>.
- [37] S.K. Yadav, N. Ito, J.E. Mindur, H. Kumar, M. Youssef, S. Suresh, R. Kulkarni, Y. Rosario, K.E. Balashov, S. Dhib-Jalbut, et al., Fecal Lcn-2 level is a sensitive biological indicator for gut dysbiosis and intestinal inflammation in multiple sclerosis, *Front. Immunol.* 13 (2022), 1015372, <https://doi.org/10.3389/fimmu.2022.1015372>.
- [38] S. Han, J. Zhuang, Y. Pan, W. Wu, K. Ding, Different characteristics in gut microbiome between advanced adenoma patients and colorectal cancer patients by metagenomic analysis, *Microbiol. Spectr.* 10 (2022), e0159322, <https://doi.org/10.1128/spectrum.01593-22>.
- [39] A. Pisani, P. Rausch, C. Bang, S. Ellul, T. Tabone, C.M. Cordina, G. Zahra, A. Franke, P. Ellul, Dysbiosis in the gut microbiota in patients with inflammatory bowel disease during remission, *Microbiol. Spectr.* 10 (2022), e0061622, <https://doi.org/10.1128/spectrum.00616-22>.
- [40] J. Hu, J. Yang, L. Chen, X. Meng, X. Zhang, W. Li, Z. Li, G. Huang, Alterations of the gut microbiome in patients with pituitary adenoma, *Pathol. Oncol. Res.* 28 (2022), 1610402, <https://doi.org/10.3389/pore.2022.1610402>.
- [41] B. Liu, D. Ye, H. Yang, J. Song, X. Sun, Y. Mao, Z. He, Two-sample mendelian randomization analysis investigates causal associations between gut microbial genera and inflammatory bowel disease, and specificity causal associations in ulcerative colitis or crohn's disease, *Front. Immunol.* 13 (2022), 921546, <https://doi.org/10.3389/fimmu.2022.921546>.
- [42] X. Tang, W. Wang, G. Hong, C. Duan, S. Zhu, Y. Tian, C. Han, W. Qian, R. Lin, X. Hou, Gut microbiota-mediated lysophosphatidylcholine generation promotes colitis in intestinal epithelium-specific Fut2 deficiency, *J. Biomed. Sci.* 28 (2021) 20, <https://doi.org/10.1186/s12929-021-00711-z>.
- [43] A. Sharma, S. Szymczak, M. Rühlemann, S. Freitag-Wolf, C. Knecht, J. Enderle, S. Schreiber, A. Franke, W. Lieb, M. Krawczak, et al., Linkage analysis identifies novel genetic modifiers of microbiome traits in families with inflammatory bowel disease, *Gut Microb.* 14 (2022), 2024415, <https://doi.org/10.1080/19490976.2021.2024415>.
- [44] H. Zhao, X. Jin, Causal associations between dietary antioxidant vitamin intake and lung cancer: a Mendelian randomization study, *Front. Nutr.* 9 (2022), 965911, <https://doi.org/10.3389/fnut.2022.965911>.
- [45] H. Yi, G. Talmon, J. Wang, Glutamate in cancers: from metabolism to signaling, *J. Biomed. Res.* 34 (2019) 260–270, <https://doi.org/10.7555/JBR.34.20190037>.
- [46] M. Yan, X. Li, C. Sun, J. Tan, Y. Liu, M. Li, Z. Qi, J. He, D. Wang, L. Wu, Sodium butyrate attenuates AGEs-induced oxidative stress and inflammation by inhibiting autophagy and affecting cellular metabolism in THP-1 cells, *Molecules* 27 (2022) 8715, <https://doi.org/10.3390/molecules27248715>.
- [47] T. Li, A. Le, Glutamine metabolism in cancer, *Adv. Exp. Med. Biol.* 1063 (2018) 13–32, https://doi.org/10.1007/978-3-319-77736-8_2.
- [48] C. Liu, D. Fan, Q. Lei, A. Lu, X. He, Roles of resolvins in chronic inflammatory response, *Int. J. Mol. Sci.* 23 (2022), 14883, <https://doi.org/10.3390/ijms232314883>.
- [49] N. Arjomand Fard, M. Bording-Jorgensen, E. Wine, A potential role for gut microbes in mediating effects of omega-3 fatty acids in inflammatory bowel diseases: a comprehensive review, *Curr. Microbiol.* 80 (2023) 363, <https://doi.org/10.1007/s00284-023-03482-y>.
- [50] Human Microbiome Project Consortium, Structure, function and diversity of the healthy human microbiome, *Nature* 486 (2012) 207–214, <https://doi.org/10.1038/nature11234>.